

Optical control of the spin-Hall effect in a two-dimensional hole gas

Simone Rossi,¹ Valentina Caprotti,¹ Andrea Filippi,¹ Emiliano Bonera,¹
Jacopo Pedrini,¹ Roberto Raimondi,² Maksym Myronov,³ and Fabio Pezzoli^{1,*}

¹*Dipartimento di Scienza dei Materiali, Università degli Studi di
Milano-Bicocca and BiQuTe, Via R. Cozzi 55, 20125 Milano, Italy*

²*Dipartimento di Matematica e Fisica, Università Roma Tre, Via della Vasca Navale 84, 00146 Roma, Italy*

³*Department of Physics, The University of Warwick, Gibbet Hill Road, CV4 7AL Coventry, UK*

Relativistic effects influence the motion of charged particles in solids by intertwining spin and momentum. The resulting phenomena exhibit rich and intriguing properties that can unveil radically new quantum devices. In this context, the two-dimensional hole gas formed in group IV heterostructures is a particularly promising platform, owing to a notable spin-orbit coupling. However, the exploitation of spin-momentum locking and precise manipulation of spin currents has remained elusive thus far. Here we use the modulation-doping technique to break inversion symmetry at novel $\text{Ge}_{1-x}\text{Sn}_x/\text{Ge}$ interfaces and explore spin-orbit phenomena in the emergent Rashba-coupled hole gases. Magneto-optical investigations demonstrate the unusual establishment of a staggered band alignment with carrier lifetime in the ns range. Optical spin orientation is then leveraged to directly inject spin-polarized currents in the Rashba-split 2D gas. Spin-to-charge conversion is shown to genuinely occur at the staggered gap through the inverse spin-Hall effect. This provides unprecedented access to low-order contributions of the spin-orbit Hamiltonian. Moreover, it leads to the startling demonstration that the spin Hall angle can be optically controlled by modifying the Rashba coupling through the photoexcitation density. $\text{Ge}_{1-x}\text{Sn}_x$ quantum wells thus offer innovative solutions and functionalities stemming from their unique spin-dependent properties and intriguing quantum phenomena at the crossroad between transport and photonic realms.

INTRODUCTION

Spin-orbit interaction is a relativistic effect that couples spin and momentum of charged particles. In solids this gives rise to the emergence of rich and intriguing spin-dependent phenomena, whose exploitation can advance the thriving field of quantum technologies.[1–3] Group IV materials may unleash tremendous opportunities in this context being a leading-edge platform perfected through decades of nanotechnology research.

Specifically, Ge-based heterostructures can confine electrons in the form of a two-dimensional (2D) Fermi system, offering an ideal playground to tailor functional properties through spin-orbit coupling (SOC). This has been exemplified by the demonstration of long spin relaxation time and large anisotropy of the electron Landé g-factor in Ge/SiGe quantum wells (QW).[4] The formation of a 2D hole gas (2DHG) in Ge QWs has also led to the demonstration of g-factor manipulation [5, 6] and exceptionally high mobilities, i.e., exceeding 10^6 cm^2/Vs . [7] Recently it has been utilized as a primer for the fabrication of hole spin qubits relevant for quantum information processing.[8, 9] Indeed, the strong SOC that pertains to the valence band allows fast quantum logic operations. At the same time, hyperfine interactions are minimized by the p -type orbital character of the hole wavefunction, thus offering a long coherence time.[10, 11]

While the introduction of an electrostatic potential through modulation doping (MOD) or a gate lead traps the 2DHG at the Ge/SiGe interface, it spontaneously breaks the structural symmetry of the system.[12] This notably generates an unusual spin texture, which stems

from Rashba spin splitting.[13–16] The latter might offer a compelling platform to develop persistent spin helix states that can be used to implement spin interconnects or quantum buses using the state-of-the-art manufacture of integrated circuits.[17, 18] Above all, such Rashba-split hole gas provides a favorable testbed to explore synthetic spin-orbit fields that sustain spin-polarized states even at zero magnetic field. These are of primary interest in the quest to control the orbital motion of carriers and to manipulate the mutual conversion between spin and charge currents via the spin galvanic (Edelstein) and spin Hall effects.[19–22] A context in which 2DHGs based on group IV materials remain vastly untapped.

In this scenario, the novel class of group IV alloys based on the heavy element Sn holds excellent spin properties.[23–25] The investigation of SOC manipulation in $\text{Ge}_{1-x}\text{Sn}_x$ heterostructures offers indeed the unique possibility to judiciously modify the system Hamiltonian by strain and bandgap engineering, thus providing radically new possibilities to implement spin-dependent functionalities beyond Ge. In addition, we anticipate that the strong light-matter interaction pertaining to Sn-based alloys [23, 26] and the flexible design introduced by SOC engineering can make $\text{Ge}_{1-x}\text{Sn}_x$ 2DHG a prominent candidate also at the leading edge between Si photonics and the burgeoning field of spin-orbitronics.[1]

In this work we leverage optical spectroscopy to explore these advanced capabilities. Specifically, we investigate the spin physics of individual p -type MOD QWs realized by embedding $\text{Ge}_{0.91}\text{Sn}_{0.09}$ layers within barriers made of elemental Ge. The formation of a 2DHG at

cryogenic temperatures is proved by magneto-transport measurements, while excitation-dependent photoluminescence (PL) provides us with the fingerprint of an unexpected staggered band lineup for L -valley electrons. A finding that advances our understanding of the electronic structure of these novel heterojunctions. Optical spin orientation is then exploited, in conjunction with external magnetic fields, to determine the spin lifetime through the Hanle effect.[24, 27] Notably, we observe spin-to-charge interconversion as a manifestation of the inverse spin-Hall (ISHE) effect in dedicated Hall-bar devices.[28–31] A result that allow us to provide a first estimation of the spin-Hall angle pertaining to this 2D system. In particular, these investigations demonstrate that heterojunctions featuring a distinct staggered gap can offer convenient control through direct laser excitation of the spin-to-charge conversion efficiency. Optical pumping has been finally utilized to unveil Rashba terms in the spin-orbit Hamiltonian that are linear in momentum. Such low-order component remained concealed to recent experimental observations of 2D-SOC systems.[14–16, 32]

These findings open new research directions for the generation of pure spin currents and introduce group IV heterostructures as a practical platform for the future implementation of spin-orbitronic and spin-optronic functionalities.

RESULTS AND DISCUSSION

Electronic and optical properties of 2DHGs in $\text{Ge}_{1-x}\text{Sn}_x$ QWs

Figure 1a shows the cross-sectional layout of the epitaxial layers forming the p -type MOD device along with an optical image of a representative geometry of the Hall bar used in this work. The thickness of the Ge spacer separating the $\text{Ge}_{0.91}\text{Sn}_{0.09}$ QW from the Ge:B layer is of about 20 (S-20), 100 (S-100) or 150 (S-150) nm. See the Methods section for details about the sample growth and device fabrication.

At first, magnetotransport investigations have been conducted through resistivity and Hall effect measurements at temperatures varying in the 0.3–3.6 K range. The main results are shown in Figure 1b for sample S-20. While the transverse resistance (R_{xy}) shows well-defined plateaus at high magnetic fields, distinct Shubnikov-de Haas oscillations are clearly visible in the longitudinal resistivity (ρ_{xx}) over the whole temperature range, thus confirming the formation of a high-mobility 2DHG in the $\text{Ge}_{0.91}\text{Sn}_{0.09}$ QW. The visibility of the oscillation pattern let us expect that the gas can withstand high temperatures operation. This is corroborated by results on similar structures where 2DHGs were singled out up to 5 K.[33] At 300 mK a 2DHG carrier density of $1.7 \times 10^{11} \text{cm}^{-2}$ and mobility of $\approx 37300 \text{cm}^2 \text{V}^{-1} \text{s}^{-1}$ was

derived, suggesting negligible conduction through parasitic channels. Notably, the biaxial compressive strain in the QW plane shifts the light-hole states at higher energies. This reduces the orbital mixing in the valence band and ensures that only the lowest heavy-hole (HH) subbands are populated.[32, 33] Finally, in Figure 1b a double peak can be observed to arise at 1.56 T ($\nu = 9$), which can be ascribed to the Zeeman spin splitting of the HH states.[33]

After having provided a compelling proof of the formation of the 2DHG through transport data, we are well positioned to focus on light-matter phenomena arising in this novel system. The excellent quality of the samples remarkably ensures that they are sufficiently bright to allow the direct observation of the radiative emission from the individual QW. This is readily demonstrated by the temperature-dependent photoluminescence (PL) summarized in Figure 1c.

It should be noticed that the strain imparted to the $\text{Ge}_{0.91}\text{Sn}_{0.09}$ QW by the Ge-on-Si buffer has repercussions not only on transport, as previously discussed, but also on the PL. Beside lifting the valence band degeneracy, compressive strain strengthens the indirect character of the bandgap. Consequently, the peak appearing at cryogenic temperatures in Figure 1c at about 0.6 eV for sample S-20 can be ascribed to indirect transitions that involve the lowest subbands of the HH at the zone center and electrons at the L point of the Brillouin zone.[34, 35] Owing to the Varshni's law, this spectral feature, termed HH1 – cL1, redshifts as the temperature increases. The same behavior holds for the samples S-100 and S-150 (see the inset of Figure 1c).

$\text{Ge}_{1-x}\text{Sn}_x$ heterojunctions have been developed only very recently as a means of band engineering, and various contrasting possibilities have been put forward thus far to describe offsets and discontinuities in the individual bands. Specifically, the conduction band lineup at $\text{Ge}_{1-x}\text{Sn}_x/\text{Ge}$ heterointerfaces has remained undetermined with debated configurations that have been often derived from theoretical predictions, despite the lack of accurate calculation parameters. Presently, conflicting straddling (type I) [33, 34, 36] and staggered (type II) [37] alignments have been suggested. In the following, we demonstrate that optical spectroscopy can be instrumental to experimentally resolve such crucial ambiguities.

In type I heterostructures, like the prototypical $\text{Ge}/\text{Si}_{0.85}\text{Ge}_{0.15}$ QWs,[4, 38, 39] electrons and holes are both confined in the same QW layer. Conversely, a type II band lineup as in Si/Ge QWs isolates carriers at opposite sides of the interface according to the sign of the charge,[40] thereby forming spatially indirect excitons alongside a dipole layer. The latter causes band-bending in the vicinity of the junction, whose steepness can be eventually modified through optical excitation. An increase of the pump power raises the carrier population, thus strengthening the electrostatic potential across

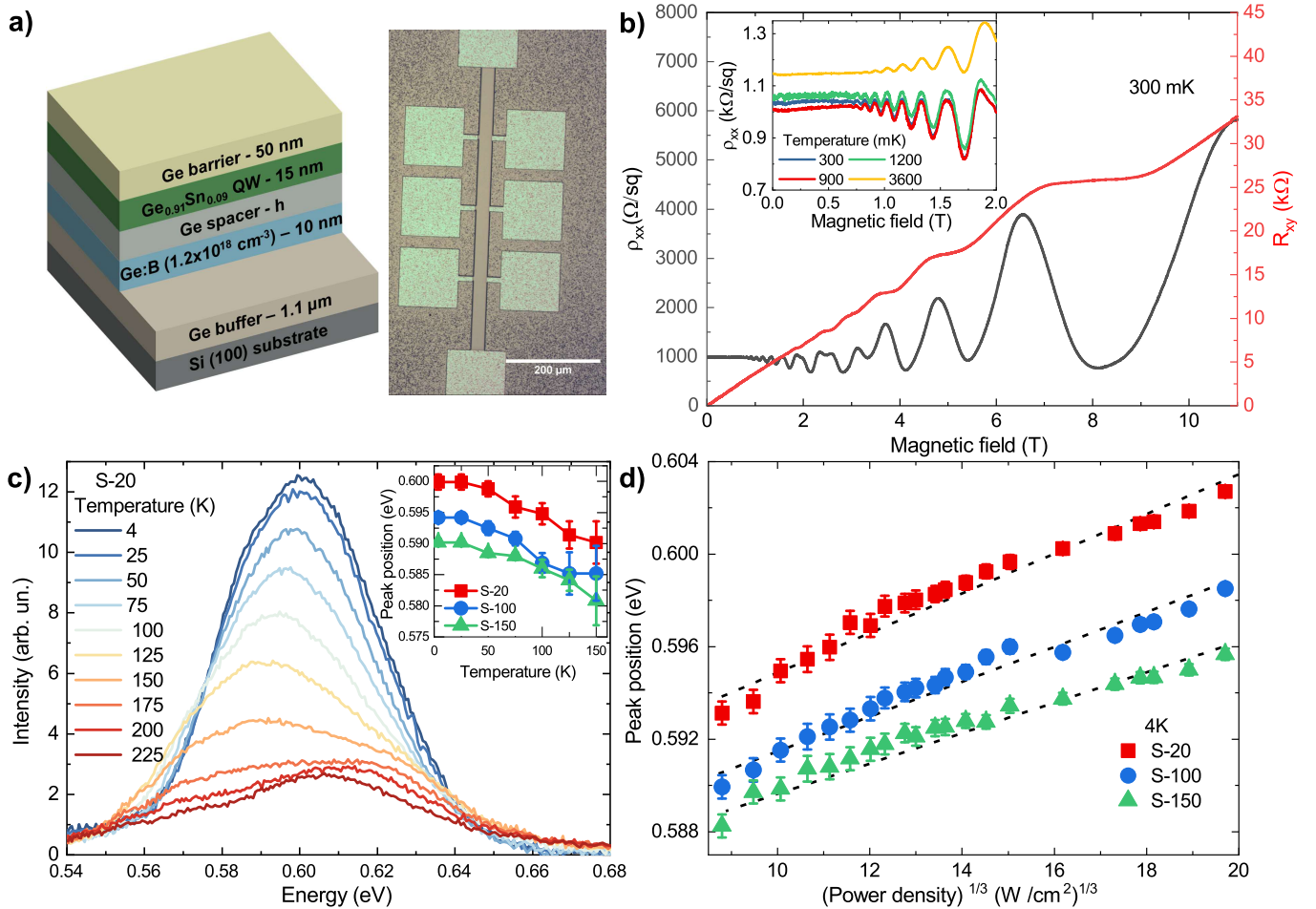


FIG. 1. (a) Schematic representation of the heterostructure. The Ge spacer thickness (h) is changed between the three samples: $h = 20$ nm for S-20, $h = 100$ nm for S-100 and $h = 150$ nm for S-150. On the right an optical image of a Hall bar structure patterned for transport and optical measurements. (b) Magnetotransport results at 300 mK showing Shubnikov-De Haas oscillations, i.e., the fingerprint of two-dimensional hole gas formation, as well as plateaus in the Hall resistance. The oscillations are found in the whole temperature range of 0.3 – 3.6 K. (c) Photoluminescence of S-20 in the temperature range 4 - 225 K under an illumination power density of 3.40 kW/cm². (d) Peak position versus the third root of excitation power density showing a linear behavior.

the interface. This, in turns, enlarges the quantization energy so that a blueshift of the PL can be expected. The increase of the emission energy with the third root of the excitation density has been shown to provide a compelling proof of the establishment of such staggered lineup.[41–44]

In the following, we utilize the spectral shift analysis to investigate the band alignment at the Ge_{0.91}Sn_{0.09}/Ge heterointerface. Figure 1d demonstrates that a pump-induced blueshift can be consistently observed for all the samples. Since many-body effects and heating from the laser excitation would have rather caused a redshift, owing to band-gap renormalization and temperature-induced bandgap narrowing, we can safely conclude that the unambiguous high-energy drift reported in Figure 1d demonstrates the emergence of state filling. This is further confirmed by the observation that the energy shift

nically scales with the third root of the excitation power. Such remarkable finding makes a strong case for a type II heterostructure, in which the 2DHG is confined in the Ge_{0.91}Sn_{0.09} QW and is surrounded by Ge barriers that become negatively charged under out-of-equilibrium conditions.

It can be further noticed that at a fixed pump power, the samples exhibit an energy increase of the HH1 – cL1 peak as the thickness of the Ge spacer is reduced (see Figure 1d and the inset of Figure 1c). The reduction of the distance between the Ge:B doped region and the QW facilitates indeed trapping of the extrinsic charges by the well and increases the exerted electric field. This enlarges the density of holes that reside in the QW, progressively filling up the lowest energy states as the spacer is thinned down. This process forces photo-generated carriers to occupy higher energy levels, eventually yielding the ob-

served blue-shift of the PL as a function of the width of the Ge spacer. This finding further supports the presence of a 2DHG in the QWs and suggest that both the MOD structure and the photoinduced state filling can contribute to the overall blueshift of the PL.

Spin-resolved properties

Given the intriguing possibility of addressing the emission of a single $\text{Ge}_{0.91}\text{Sn}_{0.09}$ QW, we can hereafter utilize optical spin orientation [45] and gather optical access to the fundamental spin-dependent properties of the 2DHG.

To this purpose, we will evaluate the spin lifetime (T_s) at cryogenic temperatures, namely 4 K, by leveraging the recent extension of the Hanle effect to group IV materials achieved through magneto-PL.[24] We therefore conducted experiments in a Voigt geometry, that is, the magnetic field (B) being perpendicular to the spin quantization axis. The latter is defined by the light propagation path being parallel to the growth direction, hence normal, in our configuration, to the QW plane.

Figure 2a shows that at a specific excitation power density of 3.4 kW/cm^2 , all the samples demonstrate a sizable circular polarization degree (ρ). This is due to radiative recombination events involving spin-polarized carriers generated through the process of optical spin injection.[23, 46, 47]. In particular, at zero field, sample S-20 demonstrates a $\rho_0 \equiv \rho(B = 0)$ of about 9%, whereas the polarization degree is higher for the other two samples and equal to $\sim 12\%$. This modification of ρ_0 can be likely ascribed to the inherent p -MOD structure. The structural asymmetry that originates from the one-side modulation doping leads to the emergence of the so-called Rashba effect.[48, 49] This acts as a perturbation to the spin ensemble, which causes a loss of the polarization degree, thereby shortening the spin relaxation time (T_1) and, in turns, decreases the observable ρ_0 . [50] This mechanisms becomes more pronounced when the strength of the effective electric field is increased by moving the doping layer closer to the QW as in S-20.

Notably, $\rho(B)$ of all the samples decays by increasing the strength of the field and gets completely washed out above $\sim 20 \text{ mT}$. Such a well-defined behavior is fully consistent with the Lorentzian lineshape expected for the Hanle effect, i.e., $\rho(B) = \rho_0 / [1 + (\Omega T_s)^2]$, [27] where the Larmor precession frequency $\Omega = (g\mu_B B)/\hbar$ depends on the strength of the magnetic field and the g factor through the Bohr magneton (μ_B) and the reduced Planck constant (\hbar).

It is worth noting that a marked increase in the Hanle linewidth can be effectively induced by changing the power density of the optical pump from 0.85 to 6.80 kW/cm^2 (see the inset of Figure 2a). Using the predicted lineshape for the Hanle curves [24] and the experimental

g -factor of 1.4828 from Ref. [23], we derived the change of T_s upon the excitation power. These results are summarized in Figure 2b and readily manifests that a pump-induced shortening of the spin lifetime can occur in all the $\text{Ge}_{0.91}\text{Sn}_{0.09}/\text{Ge}$ QWs. We emphasize that the spin lifetime extracted from the Hanle curve arises from the intertwined contributions of the spin-relaxation time and the carrier lifetime (τ), being $1/T_s = 1/T_1 + 1/\tau$. In particular, the observation of circularly polarized emission allows us to conclude that T_1 is practically longer than τ . Consequently, any change in T_s is mainly governed by modifications of the carrier lifetime.[24, 46]

The type-II band alignment inhibits the coexistence of opposite charges within the same spatial layer. As a result, a reduced recombination probability and, in turn, a lengthening of the carrier lifetime can be expected in $\text{Ge}_{0.91}\text{Sn}_{0.09}/\text{Ge}$ QWs as compared to the bulk. Consistently, the values of the spin lifetime demonstrated in Figure 2b are in the ns range, which is markedly longer than the sub-ns regime reported by previous experimental works on epitaxial bulk-like films, provided that a Sn molar fraction similar to the one studied here is considered.[24, 51] The carrier lifetime obtained via magneto-PL compares favorably also with recent results on $\text{SiGeSn}/\text{GeSn}/\text{SiGeSn}$ QWS.[52] Moreover, it can be noticed that the longest lifetime shown in Figure 2b pertains to sample S-20. This QW owns the thinnest Ge spacer, i.e., the deepest confining potential, which ensures better bound states. More importantly, the large carrier lifetime of sample S-20 can also concur with the Rashba field to lower the value of ρ_0 as the polarization degree is ultimately dictated, under steady state conditions, by the ratio T_1/τ . [46, 47, 53]

The monotonic power-dependent decrease of T_s and its marked effect observed in Figure 2b also stems from the type II nature of the band lineup in $\text{Ge}_{0.91}\text{Sn}_{0.09}/\text{Ge}$ QWs. The growth of the dense non-equilibrium distribution of carriers induced by enlarging the fluence of the optical pump progressively fills higher energy states of the QW, which are characterized by a larger penetration of the associated wave functions into the adjacent barrier layers. This process is of greater importance for QWs having a larger confinement energy and improves the otherwise small spatial overlap between the electrons and holes that are confined at the opposite sides of the hetero-interface. Eventually, this mechanism increments the oscillator strength governing the optical transitions and shortens the radiative recombination time as observed in Figure 2b.[54, 55] In S-20 the increase of the power density causes indeed the most pronounced shortening of the spin lifetime as T_s is almost halved being reduced from 1.8 ns until it equals the data of the other two QW samples at about 1 ns (see Figure 2b).

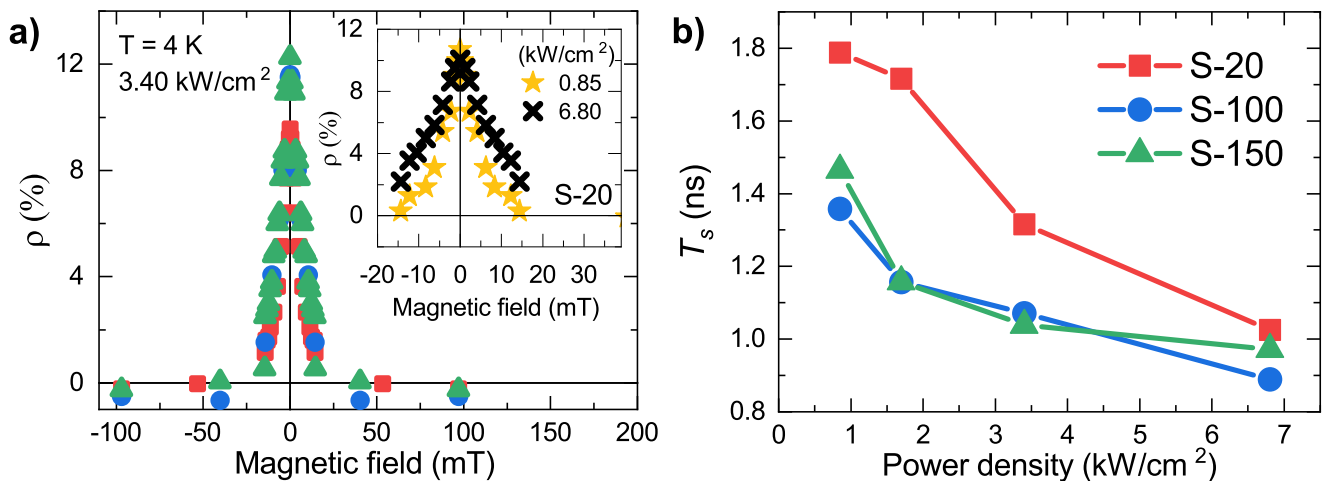


FIG. 2. (a) Hanle curves of the $\text{Ge}_{0.91}\text{Sn}_{0.09}/\text{Ge}$ QW samples under an illumination of 3.40 kW/cm^2 . Data pertaining to sample S-20, S-100 and S-150 are shown as red squares, blue dots and green triangles, respectively. The inset shows Hanle curves of sample S-20 in a restricted region of the magnetic field at a power density of 0.85 (yellow stars) or 6.80 kW/cm^2 (black crosses). All the data are mirrored to negative magnetic fields to show the characteristic Lorentzian shape pertaining to the Hanle effect. (b) Spin lifetime (T_s) derived from the Hanle curves measured at various illumination conditions. All the measurements were performed at a temperature of 4K using a right-handed circularly polarized laser with photon energy of 1.16 eV .

Optical control of the inverse Spin-Hall effect

The presence of a structural inversion asymmetry, due to the one-sided MOD, offers the possibility to study the emergence of advanced phenomena in a 2DHG framework. Specifically, the Rashba-induced SOC, which is inherently associated with a spin texture in momentum space, can be leveraged to optically induce spin-to-charge interconversion via ISHE.

Figure 3a shows the experimental geometry utilized to demonstrate this process in the type II $\text{Ge}_{0.91}\text{Sn}_{0.09}/\text{Ge}$ heterostructure. A circularly polarized laser beam is steered along the normal (hereafter versor \hat{z}) to the Hall-bar surface, i.e., the QW plane. By labeling the Bloch states according to the total angular momentum (J) and its projection onto the z axis (J_z), it can be easily shown that, by virtue of the selection rules, inter-band transitions generate electron and heavy hole ensembles holding the same density and the same out-of-plane spin orientation.[27, 53] The latter can be either parallel or antiparallel to the direction of light propagation and is defined by the helicity of the laser. For example, a right-handed σ^+ pump promotes electrons to $|J; J_z\rangle = |1/2; -1/2\rangle$ conduction states, while injecting heavy holes into $|3/2; -3/2\rangle$ states.

The application of an electric field along the longitudinal (main) channel of the device will then cause the drift within the QW plane of the photogenerated spin-polarized carriers. The resulting electron and heavy hole spin currents stem from the anticommutator of velocity and spin [56] and flow in opposite directions, following the relative motion of the charged species. It should

be noted, however, that these two contributions to the overall spin current will not cancel out because of the different magnitude of J_z . Moreover, photoexcitation from light hole states, which is accessible in our experimental conditions, results in the same spin orientation of the HHs, while reducing the overall electron spin polarization in the conduction band. This ultimately ensures that holes drag longitudinally a net spin angular momentum. Such mechanisms, in turns, generates through spontaneous ISHE a genuine flow of charges and a voltage drop at the transverse (side) channel, V_T , that can be measured across a load resistor via standard lock-in techniques (see Methods for details).[30, 57] The sign of V_T is indeed consistent with positive charge carriers involved in the transport process.

To correct for spurious effects and to determine the unique spin-related components of the electro-optical signal, we single out the helicity-dependent photovoltage (HDP), that is, the difference between the ISHE voltage, V_T^+ and V_T^- , generated in the resistive side arm under right- and left-handed circularly polarized excitation, respectively. Fig. 3b summarizes the HDP obtained for three different laser fluences by sweeping the current in the $\pm 100 \mu\text{A}$ interval. As expected for the ISHE (see Methods), HDP demonstrates a sign inversion when the current direction is reversed. Moreover, a linear dependence of the ISHE photovoltage on the longitudinal current can be observed over a wide range of the excitation conditions. All these findings provide a compelling demonstration of the spin-to-charge interconversion occurring in the p -MOD structure.

It should be noted that when the power density is in-

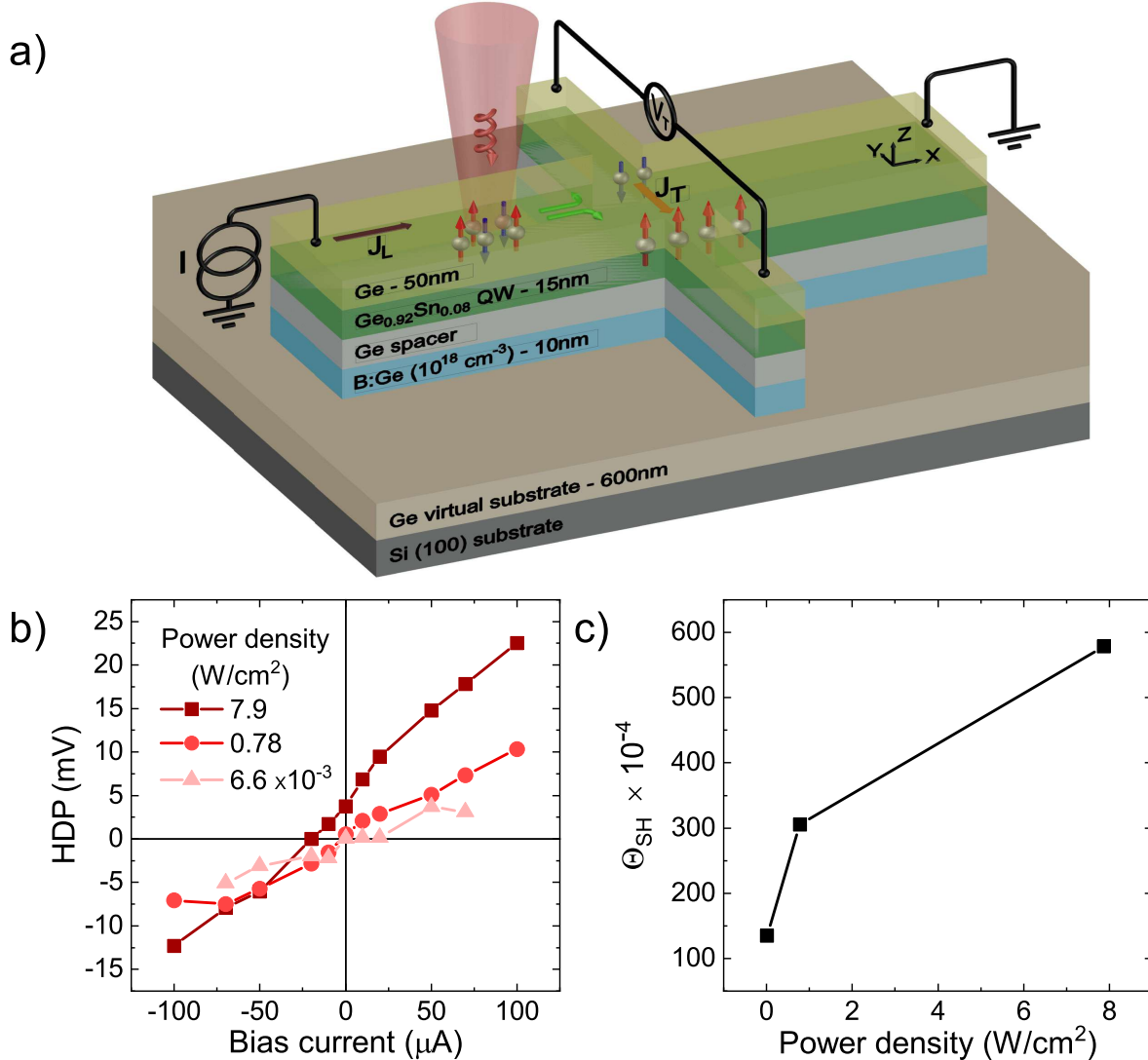


FIG. 3. : (a) Sketch of the set-up used for the measurement of the inverse spin-Hall effect (ISHE). The transverse photovoltage (V_T) is measured across the side channel by a lock-in amplifier connected to a load resistance. (b) The difference between the ISHE voltage generated in the transverse channel of the sample S-150 under right- and left-handed circularly polarized excitation provides the helicity-dependent photovoltage, HDP, reported here as a function of the bias current for three different illumination power densities. (c) Spin-Hall angle derived from the HDP data as a function of illumination.

creased to 8 W/cm^2 (dark-red squares in Fig. 3b), there still exists a residual HDP of approximately 5 mV even in complete absence of the longitudinal bias. This negligible offset can be regarded as the onset of laser-induced heating effects. The HDP measured as a function of the longitudinal current, in combination with the value of the spin polarization obtained by the optical spin orientation experiments, enabled us to finally extract the spin-Hall angle θ_{SH} , i.e., the figure of merit for the efficiency of the spin-to-charge interconversion process (see Methods). As shown in Figure 3c, the strength of the SHE increases monotonically with the power density going from 130×10^{-4} to almost 600×10^{-4} , when the

excitation is increased from 7×10^{-3} to 8 W/cm^2 .

A quick glance at table I enables us to conclude that 2DHG in staggered $\text{Ge}_{0.91}\text{Sn}_{0.09}/\text{Ge}$ stands out as a spintronic candidate, outperforming other heterostructures, particularly those consisting of group IV semiconductors. The $\text{Ge}_{0.91}\text{Sn}_{0.09}/\text{Ge}$ QW demonstrates indeed a $10x$ - $60x$ efficiency increase compared to bulk Ge, and, under comparable pump conditions, a two-fold improvement with respect to $\text{Ge}_{0.95}\text{Sn}_{0.05}$ epilayers.[61] Such distinct advantage is in line with (i) the enlarged SOC caused by alloying Ge with the heavier element Sn, and (ii) the Rashba-induced spin-splitting stemming from the structural inversion asymmetry.

TABLE I. Spin-Hall angle θ_{SH} for different materials. The temperature at which the spin-Hall angle is extracted is reported along with the bibliographic reference and the relevant charge species (electron: e, or hole: h) involved in the process.

Material	θ_{SH}	Temperature (K)	charge	Reference
GaAs	$5\text{-}200 \times 10^{-4}$	300	e	[30]
Si	1×10^{-4}	300	e	[58]
Ge	$2\text{-}11 \times 10^{-4}$	20-300	e	[59, 60]
Ge _{0.95} Sn _{0.05}	$4 \times 10^{-5} - 3 \times 10^{-1}$	300	e	[61]
Ge _{0.91} Sn _{0.09} /Ge QW	$130 - 600 \times 10^{-4}$	4	h	This work

Besides an efficient spin-to-charge conversion, Figure 3c demonstrates the unrivaled benefit offered by the type-II Ge_{0.91}Sn_{0.09}/Ge QW, that is, the practical control of θ_{SH} through optical excitation. The magneto-optical investigations, discussed previously, have shown that the laser fluency systematically modifies the band-bending and state filling because of the pump-induced reinforcement of the potential drop across the hetero-interface. According to $k \cdot p$ theory, the field gradient enters into the Rashba coefficient α_R , which couples in the Rashba Hamiltonian the spin Pauli matrices to the momentum and determines the strength of the SOC exerted on the 2DHG confined in the valence band of the QW. [62] It is thus reasonable to conclude that optical pumping in staggered heterostructures can modify, by means of carrier accumulation and state filling effects, the spin-orbit Hamiltonian that governs spin splitting and spin transport, ultimately introducing a viable and unique approach to engineer the Rashba physics occurring in a 2DHG, as shown by Figure 3c.

Finally, it is instructive to connect these ISHE results with the theory of the injection of spin currents at Rashba interfaces, as established within the framework of the inverse Edelstein effect (IEE).[63, 64] By neglecting, to a first approximation, the asymmetric confining potential of the MOD-QW, we can assume that the photogenerated spins are homogeneously distributed within the illuminated volume, defined by the circular spot of the laser (diameter $d \simeq 50\mu\text{m}$) and the thickness of the Ge_{1-x}Sn_x QW. The latter being smaller than the light penetration depth. Under such constraints and through the action of the longitudinal electric field, we can assume the establishment of a 3D flux density, j_s , given by the flow of the spin-polarized holes along the path length d . A transverse charge current, j_c , eventually manifests itself within the 2D Rashba-split hole gas. Such a conversion process is conceptually equivalent to the well-known IEE occurring in spin pumping experiments, where electrons are injected from a ferromagnetic contact into a nonmagnetic layer, whose thickness is smaller than the spin diffusion length, hence:[65, 66]

$$j_c = \frac{d}{2} \theta_{SH} j_s \quad (1)$$

Similarly, this relationship can be recast in terms of

the Rashba coefficient as:[65, 66]

$$j_c = \alpha_R \frac{\tau_S^h}{\hbar} j_s \quad (2)$$

By assuming a spin-relaxation time for holes (τ_S^h) between 2 and 20 ps [32, 67] and by combining Eqs 1 and 2, we can estimate for p-MOD Ge_{0.91}Sn_{0.09} QWs a linear coefficient α_R in the 0.1-5 meV Å range. This appears to be compatible with the value of the Rashba coefficient derived within the Kane model, e.g., for electrons[62]. Indeed, $\alpha_R = 0.5 \text{ meV Å}$ is obtained using the experimental energy gap ($\sim 0.6 \text{ eV}$), the split-off (0.44 eV) and the electric field (25 kV/cm) taken from band profile simulations [68] and evaluating the $k \cdot p$ matrix element ($\sim 1.84 \text{ eV Å}$) at the Sn molar fraction of the QW according to Ref. [35].

It should be noted that, within the Luttinger formalism, the SOC Hamiltonian of HHs should solely retain the Rashba coefficient of the k -cubic component.[56, 69] Yet, refined theoretical investigations have established the existence of a Rashba term that is linear in k and originates from bulk inversion asymmetry.[62] Although this Hamiltonian contribution is small and usually negligible, it can be expected to become important in the low-density regime, where the relative weight of the k -cubic Rashba is strongly reduced.[62] While the linear Rashba coefficient for HH has not been experimentally and theoretically addressed in Ge_{1-x}Sn_x alloys thus far, we can nevertheless find reassurance of the accuracy of our derivation by the satisfactory comparison with recent theoretical predictions set out for HHs in QWs consisting of elemental Ge.[70, 71] Even for Ge QWs, indeed, the experimental determination of the linear α_R remains beyond the grasp of transport experiments, whose resolution is practically limited to higher-order cubic terms.[14, 15, 32]

The informative role of optical investigations on the k -linear Rashba coefficient therefore unlocks intriguing properties of 2DHGs pertaining to group IV heterostructures and holds the potential to stimulate future studies on the unconventional SOC at type-II interfaces.

CONCLUSION

We have introduced an all-optical investigation of p -type MOD $\text{Ge}_{0.91}\text{Sn}_{0.09}/\text{Ge}$ QWs. These heterostructures are found to remarkably host a staggered band-edge alignment, which offers an original platform for the investigation of the rich spin physics emerging in a Rashba-split hole gas. We applied, within the context of the well-consolidated continuous-wave PL, the Hanle effect to gather information on the carrier dynamics. Specifically, the magneto-optical investigation demonstrated that quantum confinement in a type-II heterostructure results in a spatial indirect nature of the excitonic recombination, which manifests itself as a few-ns-long carrier lifetime. Moreover, the structural inversion asymmetry encoded in the MOD epitaxial architecture lifts the spin degeneracy of the band structure without requiring external magnetic fields. The resulting spin texture is enhanced by the tunable SOC introduced by alloying Ge with Sn and by the additional degree of freedom offered by the low dimensionality. Such properties constitute an interesting playground to address intriguing phenomena such as spin-to-charge interconversion via ISHE. Our experiments demonstrate that a 2DHG forming at a staggered $\text{Ge}_{1-x}\text{Sn}_x/\text{Ge}$ heterojunction permits the optical reconfiguration of the Rashba Hamiltonian and ensures full control over the the spin-Hall angle. The ability to create a robust spin current and spin-to-charge conversion through a contact-less optical approach in a 2DHG is indeed intriguing and highly desirable because it offer the unprecedented access to the Rashba term in the HH SOC Hamiltonian that is linear in the in-plane wave vector. Specifically, the application of $\text{Ge}_{0.91}\text{Sn}_{0.09}/\text{Ge}$ QWs can pave the way to future explorations of electro-optical manipulation of spins in quantum technologies requiring SOC control with the notable addition of a sizable spin-photon interaction.

METHODS

Sample growth and device processing Three samples are grown in a ASM Epsilon 2000 industrial-type reduced-pressure chemical vapor deposition system. The precursor materials are SnCl_4 and Ge_2H_6 with an overall H_2 atmosphere in the system. To avoid segregation, a common problem in systems with $\text{Sn} > 7\%$, a low growth temperature of approximately 270°C is used during the process. The Ge spacer layer thickness (h) was changed between 20, 100 and 150 nm. On each sample, we patterned Hall-bars with a Heidelberg Instrument μPG 101 laser writer. Contact metallization was performed via sputtering deposition of 100-nm-thick Pt layer, while a wet etch in $\text{H}_2\text{O}_2 : \text{HCl} : \text{H}_2\text{O}$ (1 : 1 : 20) was used to finalize the mesa. For the ISHE experiments, a dedicated set of Hall-bars with a width w of $200\ \mu\text{m}$ and a length

L of 5 mm was fabricated, this requirement is necessary due to the laser spot dimension.

Optical measurements PL spectra were measured at 4K under the excitation of a right-handed circularly-polarized Nd : YVO₄ laser at 1064 nm (1.165 eV). The laser spot diameter on the sample surface was approximately $50\ \mu\text{m}$. [72] The polarization of the PL was analyzed using a linear polarizer and a quarter-waveplate. The degree of circular polarization, which is a measure of the different intensity between the right- (I^+) and left- (I^-) handed circularly polarized components of the PL was determined by performing a full Stokes analysis (see Refs. [47, 73] and therein for details). The measurement of the PL intensity was conducted by coupling a monochromator to a long-wavelength single channel (In,Ga)As photodiode using a standard lock-in technique. Electrical bias was applied to the device through a Keithley source measure unit.

Inverse Spin Hall measurements We performed photovoltage measurements by connecting the side channel of the Hall bar in series to a load resistance, R_L , of 10 k Ω , while measuring the voltage drop across the latter via a lock-in amplifier. For the experiment, we then connected the main channel to a current generator. The parasitic transverse electromotive force, potentially caused by illumination-induced thermal gradients, has been minimized in the experiment by locating the optical beam in between the two side electrodes. The polarization-induced changes of the transverse voltage is thus: [30, 57]

$$\Delta V_T = V_T^+ - V_T^- = \theta_{SH} r w J_L (P^+ - P^-) \quad (3)$$

where θ_{SH} , r and J_L are the spin Hall angle, the resistivity of the sample, the longitudinal current density (the longitudinal current over the cross-sectional area), while P^+ and P^- are the carrier spin polarizations under σ^+ and σ^- excitation, respectively. Knowing the circular polarization degree through optical spin orientation measurements, ρ , we can retrieve the carrier spin polarization $P^+ = 2\rho$. From the circuit, we extract the helicity-dependent photovoltage, HDP, generated across the sample as:

$$\text{HDP} = \frac{R_S}{R_L} \Delta V_T \quad (4)$$

where R_L is the load resistance and R_S is the resistance of the sample. Due to the very low illumination power density (at least three orders of magnitude with respect to the PL measurements), R_S results from the fit of I-V curve under dark condition and accounts to 210 k Ω at 4 K.

ACKNOWLEDGMENTS

The authors would like to acknowledge L. Lonobile and B.M. Ferrari for technical assistance with the measurements. F.P. acknowledges support by the Air Force Office of Scientific Research under the award number FA8655-22-1-7050.

* fabio.pezzoli@unimib.it

- [1] A. Soumyanarayanan, N. Reyren, A. Fert, and C. Panagopoulos, Emergent phenomena induced by spinorbit coupling at surfaces and interfaces, *Nature* **539**, 509 (2016).
- [2] A. Chatterjee, P. Stevenson, S. De Franceschi, A. Morello, N. P. de Leon, and F. Kuemmeth, Semiconductor qubits in practice, *Nature Reviews Physics* **3**, 157 (2021).
- [3] F. Trier, P. Noel, J.-V. Kim, J.-P. Attane, L. Vila, and M. Bibes, Oxide spin-orbitronics: spin-charge interconversion and topological spin textures, *Nature Reviews Materials* **7**, 258 (2022).
- [4] A. Giorgioni, S. Paleari, S. Cecchi, E. Vitiello, E. Grilli, G. Isella, W. Jantsch, M. Fanciulli, and F. Pezzoli, Strong confinement-induced engineering of the g factor and lifetime of conduction electron spins in Ge quantum wells, *Nature Communications* **7**, 13886 (2016).
- [5] R. Mizokuchi, R. Maurand, F. Vigneau, M. Myronov, and S. De Franceschi, Ballistic One-Dimensional Holes with Strong g-Factor Anisotropy in Germanium, *Nano Letters* **18**, 4861 (2018).
- [6] M. Myronov, P. Waldron, P. Barrios, A. Bogan, and S. Studenikin, Electric field-tuneable crossing of hole Zeeman splitting and orbital gaps in compressively strained germanium semiconductor on silicon, *Communications Materials* **4**, 104 (2023).
- [7] M. Myronov, J. Kycia, P. Waldron, W. Jiang, P. Barrios, A. Bogan, P. Coleridge, and S. Studenikin, Holes outperform electrons in group IV semiconductor materials, *Small Science* **3**, 2200094 (2023).
- [8] N. W. Hendrickx, W. I. L. Lawrie, M. Russ, F. van Riggen, S. L. de Snoo, R. N. Schouten, A. Sammak, G. Scappucci, and M. Veldhorst, A four-qubit germanium quantum processor, *Nature* **591**, 580 (2021).
- [9] G. Scappucci, C. Kloeffel, F. A. Zwanenburg, D. Loss, M. Myronov, J.-J. Zhang, S. De Franceschi, G. Katsaros, and M. Veldhorst, The germanium quantum information route, *Nature Reviews Materials* **6**, 926 (2021).
- [10] F. Braakman and P. Scarlino, Hole spin qubits work at mT magnetic fields, *Nature Materials* **20**, 1047 (2021).
- [11] N. W. Hendrickx, D. P. Franke, A. Sammak, G. Scappucci, and M. Veldhorst, Fast two-qubit logic with holes in germanium, *Nature* **577**, 487 (2020).
- [12] A. Manchon, H. C. Koo, J. Nitta, S. M. Frolov, and R. A. Duine, New perspectives for Rashba spin-orbit coupling, *Nature Materials* **14**, 871 (2015).
- [13] G. Bihlmayer, O. Rader, and R. Winkler, Focus on the Rashba effect, *New Journal of Physics* **17**, 050202 (2015).
- [14] R. Moriya, K. Sawano, Y. Hoshi, S. Masubuchi, Y. Shiraki, A. Wild, C. Neumann, G. Abstreiter, D. Bougeard, T. Koga, and T. Machida, Cubic Rashba spin-orbit interaction of a two-dimensional hole gas in a strained-Ge/SiGe quantum well, *Physical Review Letters* **113**, 086601 (2014).
- [15] C. Morrison, P. Wisniewski, S. D. Rhead, J. Foronda, D. R. Leadley, and M. Myronov, Observation of Rashba zero-field spin splitting in a strained germanium 2D hole gas, *Applied Physics Letters* **105**, 182401 (2014).
- [16] H. J. Zhao, H. Nakamura, R. Arras, C. Paillard, P. Chen, J. Gosteau, X. Li, Y. Yang, and L. Bellaiche, Purely cubic spin splittings with persistent spin textures, *Physical Review Letters* **125**, 216405 (2020).
- [17] J. D. Koralek, C. P. Weber, J. Orenstein, B. A. Bernevig, S.-C. Zhang, S. Mack, and D. D. Awschalom, Emergence of the persistent spin helix in semiconductor quantum wells, *Nature* **458**, 610 (2009).
- [18] H. Dery, Y. Song, and I. Li, Pengke and Zutic, Silicon spin communication, *Applied Physics Letters* **99**, 082502 (2011).
- [19] M. Dyakonov and V. Perel, Possibility of orienting electron spins with current, *JETP Lett.* **13**, 467 (1961).
- [20] M. I. Dyakonov and V. I. Perel, Current-induced spin orientation of electrons in semiconductors, *Physics Letters A* **35**, 459 (1971).
- [21] E. L. Ivchenko and G. E. Pikus, New photogalvanic effect in gyrotropic crystals, *JETP Lett.* **27**, 604 (1978).
- [22] J. E. Hirsch, Spin Hall effect, *Physical Review Letters* **83**, 1834 (1999).
- [23] S. De Cesari, A. Balocchi, E. Vitiello, P. Jahandar, E. Grilli, T. Amand, X. Marie, M. Myronov, and F. Pezzoli, Spin-coherent dynamics and carrier lifetime in strained $\text{Ge}_{1-x}\text{Sn}_x$ semiconductors on silicon, *Physical Review B* **99**, 035202 (2019).
- [24] E. Vitiello, S. Rossi, C. A. Broderick, G. Gravina, A. Balocchi, X. Marie, E. P. O'Reilly, M. Myronov, and F. Pezzoli, Continuous-Wave Magneto-Optical Determination of the Carrier Lifetime in Coherent $\text{Ge}_{1-x}\text{Sn}_x/\text{Ge}$ Heterostructures, *Physical Review Applied* **14**, 064068 (2020).
- [25] B. M. Ferrari, F. Marcantonio, F. Murphy-Armando, M. Virgilio, and F. Pezzoli, Quantum spin Hall phase in GeSn heterostructures on silicon, *Physical Review Research* **5**, L022035 (2023).
- [26] O. Moutanabbir, S. Assali, X. Gong, E. O'Reilly, C. A. Broderick, B. Marzban, J. Witzens, W. Du, S.-Q. Yu, A. Chelnokov, D. Buca, and D. Nam, Monolithic infrared silicon photonics: The rise of (Si)GeSn semiconductors, *Applied Physics Letters* **118**, 110502 (2021).
- [27] F. Meier and B. P. Zakharchenya, eds., *Optical orientation* (Elsevier Science Publishers, North-Holland, New York, 1984) Chap. 2.
- [28] J. Wunderlich, B. Kaestner, J. Sinova, and T. Jungwirth, Experimental observation of the spin-Hall effect in a two-dimensional spin-orbit coupled semiconductor system, *Physical Review Letters* **94**, 047204 (2005).
- [29] K. Ando, S. Takahashi, J. Ieda, H. Kurebayashi, T. Trypiniotis, C. H. W. Barnes, S. Maekawa, and E. Saitoh, Electrically tunable spin injector free from the impedance mismatch problem, *Nature Materials* **10**, 655 (2011).
- [30] N. Okamoto, H. Kurebayashi, T. Trypiniotis, I. Farrer, D. A. Ritchie, E. Saitoh, J. Sinova, J. Masek, T. Jungwirth, and C. H. W. Barnes, Electric con-

- trol of the spin Hall effect by intervalley transitions, *Nature Materials* **13**, 932 (2014).
- [31] F. Bottegoni, M. Celebrano, M. Bollani, P. Biagioni, G. Isella, F. Ciccacci, and M. Finazzi, Spin voltage generation through optical excitation of complementary spin populations, *Nature Materials* **13**, 790 (2014).
- [32] C.-T. Tai, P.-Y. Chiu, C.-Y. Liu, H.-S. Kao, C. T. Harris, T.-M. Lu, C.-T. Hsieh, S.-W. Chang, and J.-Y. Li, Strain Effects on Rashba Spin-Orbit Coupling of 2D Hole Gases in GeSn/Ge Heterostructures, *Advanced Materials* **33**, 2007862 (2021).
- [33] Y. Gul, M. Myronov, S. Holmes, and M. Pepper, Activated and Metallic Conduction in p-Type Modulation-Doped GeSn Devices, *Physical Review Applied* **14**, 054064 (2020).
- [34] C.-Y. Lin, H.-Y. Ye, F.-L. Lu, H. S. Lan, and C. W. Liu, Biaxial strain effects on photoluminescence of Ge/strained GeSn/Ge quantum well, *Optical Materials Express* **8**, 2795 (2018).
- [35] Z. Song, W. Fan, C. S. Tan, Q. Wang, D. Nam, D. H. Zhang, and G. Sun, Band structure of $\text{Ge}_{1-x}\text{Sn}_x$ alloy: a full-zone 30-band kp model, *New Journal of Physics* **21**, 073037 (2019).
- [36] L. Qian, W. J. Fan, C. S. Tan, and D. H. Zhang, Temperature enhanced spontaneous emission rate spectra in GeSn/Ge quantum wells, *Optical Materials Express* **7**, 800 (2017).
- [37] D. Stange, N. von den Driesch, D. Rainko, C. Schulte-Braucks, S. Wirths, G. Mussler, A. T. Tiedemann, T. Stoica, J. M. Hartmann, Z. Ikonc, S. Mantl, D. Grützmacher, and D. Buca, Study of GeSn based heterostructures: towards optimized group IV MQW leds, *Optics Express* **24**, 1358 (2016).
- [38] Y.-H. Kuo, Y. K. Lee, Y. Ge, S. Ren, J. E. Roth, T. I. Kamins, D. A. B. Miller, and J. S. Harris, Strong quantum-confined Stark effect in germanium quantum-well structures on silicon, *Nature* **437**, 1334 (2005).
- [39] M. Bonfanti, E. Grilli, M. Guzzi, M. Virgilio, G. Grosso, D. Chrastina, G. Isella, H. von Kaenel, and A. Neels, Optical transitions in Ge/SiGe multiple quantum wells with Ge-rich barriers, *Physical Review B* **78**, 041407 (2008).
- [40] F. Schaeffler, High-mobility Si and Ge structures, *Semiconductor Science and Technology* **12**, 1515 (1997).
- [41] N. N. Ledentsov, J. Böhrer, M. Beer, F. Heinrichsdorff, M. Grundmann, D. Bimberg, S. V. Ivanov, B. Y. Meltser, S. V. Shaposhnikov, I. N. Yassievich, N. N. Faleev, P. S. Kop'ev, and Z. I. Alferov, Radiative states in type-II GaSb/GaAs quantum wells, *Physical Review B* **52**, 14058 (1995).
- [42] N. Pavarelli, T. J. Ochalski, F. Murphy-Armando, Y. Huo, M. Schmidt, G. Huyet, and J. S. Harris, Optical emission of a strained direct-band-gap Ge quantum well embedded inside InGaAs alloy layers, *Physical Review Letters* **110**, 177404 (2013).
- [43] D. S. Abramkin, A. K. Gutakovskii, and T. S. Shamirzaev, Heterostructures with diffused interfaces: Luminescent technique for ascertainment of band alignment type, *Journal of Applied Physics* **123**, 115701 (2018).
- [44] V. A. Timofeev, A. I. Nikiforov, A. R. Tuktamyshev, V. I. Mashanov, I. D. Loshkarev, A. A. Bloshkin, and A. K. Gutakovskii, Pseudomorphic GeSiSn, SiSn and Ge layers in strained heterostructures, *Nanotechnology* **29**, 154002 (2018).
- [45] G. Lampel, Nuclear dynamic polarization by optical electronic saturation and optical pumping in semiconductors, *Physical Review Letters* **20**, 491 (1968).
- [46] R. R. Parsons, Band-to-band optical pumping in solids and polarized photoluminescence, *Physical Review Letters* **23**, 1152 (1969).
- [47] F. Pezzoli, F. Bottegoni, D. Trivedi, F. Ciccacci, A. Giorgioni, P. Li, S. Cecchi, E. Grilli, Y. Song, M. Guzzi, H. Dery, and G. Isella, Optical spin injection and spin lifetime in Ge heterostructures, *Physical Review Letters* **108**, 156603 (2012).
- [48] Y. A. Bychkov and E. I. Rashba, Oscillatory effects and the magnetic susceptibility of carriers in inversion layers, *Journal of Physics C: Solid State Physics* **17**, 6039 (1984).
- [49] E. I. Rashba and V. I. Sheka, Symmetry of energy bands in crystals of wurtzite type: II. Symmetry of bands including spin-orbit interaction, *Fiz. Tverd. Tela: Collected Papers* **2**, 162 (1959).
- [50] S. Rossi, E. Talamas Simola, M. Raimondo, M. Acciarri, J. Pedrini, A. Balocchi, X. Marie, G. Isella, and F. Pezzoli, Optical manipulation of the Rashba effect in germanium quantum wells, *Advanced Optical Materials* **10**, 2201082 (2022).
- [51] E. Rogowicz, J. Kopaczek, J. Kutrowska-Girzycka, M. Myronov, R. Kudrawiec, and M. Syperek, Carrier dynamics in thin germanium-tin epilayers, *ACS Applied Electronic Materials* **3**, 344 (2021).
- [52] P. C. Grant, P. T. Webster, R. A. Carrasco, J. V. Logan, C. P. Hains, N. Gajowski, S.-Q. Yu, B. Li, C. P. Morath, and D. Maestas, Auger-limited minority carrier lifetime in GeSn/SiGeSn quantum well, *Applied Physics Letters* **124**, 111110 (2024).
- [53] I. Žutić, J. Fabian, and S. Das Sarma, Spintronics: Fundamentals and applications, *Review of Modern Physics* **76**, 323 (2004).
- [54] S. V. Zaitsev, A. A. Maksimov, I. I. Tartakovskii, D. R. Yakovlev, M. Bayer, and A. Waag, Radiative and non-radiative recombination in type-II ZnSe/BeTe quantum wells, *Physical Review B* **76**, 035312 (2007).
- [55] M. Baranowski, M. Syperek, R. Kudrawiec, J. Misiewicz, J. A. Gupta, X. Wu, and R. Wang, Carrier dynamics in type-II GaAsSb/GaAs quantum wells, *Journal of Physics: Condensed Matter* **24**, 185801 (2012).
- [56] B. A. Bernevig and S.-C. Zhang, Intrinsic spin Hall effect in the two-dimensional hole gas, *Physical Review Letters* **95**, 016801 (2005).
- [57] Y. Liu, J. Besbas, Y. Wang, P. He, M. Chen, D. Zhu, Y. Wu, J. M. Lee, L. Wang, J. Moon, N. Koirala, S. Oh, and H. Yang, Direct visualization of current-induced spin accumulation in topological insulators, *Nature Communications* **9**, 2492 (2018).
- [58] K. Ando and E. Saitoh, Observation of the inverse spin Hall effect in silicon, *Nature Communications* **3**, 629 (2012).
- [59] J.-C. Rojas-Sánchez, M. Cubukcu, A. Jain, C. Vergnaud, C. Portemont, C. Ducruet, A. Barski, A. Marty, L. Vila, J.-P. Attané, E. Augendre, G. Desfonds, S. Gambarelli, H. Jaffrès, J.-M. George, and M. Jamet, Spin pumping and inverse spin Hall effect in germanium, *Physical Review B* **88**, 064403 (2013).
- [60] F. Bottegoni, C. Zucchetti, S. Dal Conte, J. Frigerio, E. Carpena, C. Vergnaud, M. Jamet, G. Isella, F. Ciccacci, G. Cerullo, and M. Finazzi, Spin-Hall voltage over a large length scale in bulk germanium,

- Physical Review Letters **118**, 167402 (2017).
- [61] A. Marchionni, C. Zucchetti, F. Ciccacci, M. Finazzi, H. S. Funk, D. Schwarz, M. Oehme, J. Schulze, and F. Bottegoni, Inverse spin-Hall effect in GeSn, Applied Physics Letters **118**, 212402 (2021).
- [62] R. Winkler, *Spin-orbit Coupling Effects in Two-Dimensional Electron and Hole Systems*, Springer Tracts in Modern Physics (Springer, Berlin, Heidelberg, 2003).
- [63] V. Edelstein, Spin polarization of conduction electrons induced by electric current in two-dimensional asymmetric electron systems, Solid State Communications **73**, 233 (1990).
- [64] K. Shen, G. Vignale, and R. Raimondi, Microscopic theory of the inverse Edelstein effect, Physical Review Letters **112**, 096601 (2014).
- [65] J. C. R. Sanchez, L. Vila, G. Desfonds, S. Gambarelli, J. P. Attane, J. M. De Teresa, C. Magen, and A. Fert, Spin-to-charge conversion using Rashba coupling at the interface between non-magnetic materials, Nature Communications **4**, 2944 (2013).
- [66] J.-C. Rojas-Sánchez, S. Oyarzún, Y. Fu, A. Marty, C. Vergnaud, S. Gambarelli, L. Vila, M. Jamet, Y. Ohtsubo, A. Taleb-Ibrahimi, P. Le Fèvre, F. Bertran, N. Reyren, J.-M. George, and A. Fert, Spin to charge conversion at room temperature by spin pumping into a new type of topological insulator: α -Sn films, Physical Review Letters **116**, 096602 (2016).
- [67] C. Lange, G. Isella, D. Chrastina, F. Pezzoli, N. S. Köster, R. Woscholski, and S. Chatterjee, Spin band-gap renormalization and hole spin dynamics in Ge/SiGe quantum wells, Physical Review B **85**, 241303 (2012).
- [68] S. Birner, T. Zibold, T. Andlauer, T. Kubis, M. Sabathil, A. Trellakis, and P. Vogl, Nextnano: General purpose 3-D simulations, IEEE Transactions on Electron Devices **54**, 2137 (2007).
- [69] S. Murakami, Absence of vertex correction for the spin Hall effect in p -type semiconductors, Physical Review B **69**, 241202 (2004).
- [70] J.-X. Xiong, Y. Liu, S. Guan, J.-W. Luo, and S.-S. Li, Why experiments fail to detect the finite linear Rashba spin-orbit coupling of two-dimensional holes in semiconductor quantum wells: The case of Ge/SiGe quantum wells, Physical Review B **106**, 155421 (2022).
- [71] E. A. Rodríguez-Mena, J. C. Abadillo-Uriel, G. Veste, B. Martinez, J. Li, B. Sklénard, and Y.-M. Niquet, Linear-in-momentum spin orbit interactions in planar ge/gesi heterostructures and spin qubits, Physical Review B **108**, 205416 (2023).
- [72] F. Pezzoli, A. Giorgioni, D. Patchett, and M. Myronov, Temperature-Dependent Photoluminescence Characteristics of GeSn Epitaxial Layers, ACS Photonics **3**, 2004 (2016).
- [73] F. Pezzoli, L. Qing, A. Giorgioni, G. Isella, E. Grilli, M. Guzzi, and H. Dery, Spin and energy relaxation in germanium studied by spin-polarized direct-gap photoluminescence, Physical Review B **88**, 045204 (2013).